

Ge_{1-x}Sn_x Alloy Quantum Dots with Composition- Tunable Energy Gaps and Near-Infrared Photoluminescence

*Venkatesham Tallapally,¹ Tanner A. Nakagawara,² Denis O. Demchenko,³ Ümit Özgür,² and
Indika U. Arachchige^{1*}*

¹Department of Chemistry, Virginia Commonwealth University, Richmond, Virginia 23284,
United States

²Department of Electrical and Computer Engineering, Virginia Commonwealth University,
Richmond, Virginia 23284, United States

³Department of Physics, Virginia Commonwealth University, Richmond, Virginia 23284, United
States

Electronic Supplementary Information

Table S1. The molar ratio of GeI₂, SnCl₂, and n-BuLi used in the synthesis of 3.3 ± 0.5–5.9 ± 0.8 nm Ge_{1-x}Sn_x (x = 1.5 – 20.6%) alloy QDs. The total moles of GeI₂ and SnCl₂ was fixed at 0.6 mmol.

Sample	GeI ₂ (mmol)	SnCl ₂ (mmol)	n-BuLi (mmol)
Ge _{0.985} Sn _{0.015}	0.591	0.0090	1.48
Ge _{0.981} Sn _{0.019}	0.5886	0.0114	1.46
Ge _{0.973} Sn _{0.027}	0.5838	0.0162	1.43
Ge _{0.966} Sn _{0.034}	0.5796	0.0204	1.42
Ge _{0.958} Sn _{0.042}	0.5748	0.0252	1.40
Ge _{0.944} Sn _{0.056}	0.5664	0.0336	1.38
Ge _{0.936} Sn _{0.064}	0.5619	0.0381	1.36
Ge _{0.921} Sn _{0.079}	0.5526	0.0474	1.34
Ge _{0.909} Sn _{0.091}	0.5454	0.0546	1.30
Ge _{0.888} Sn _{0.112}	0.5328	0.0672	1.25
Ge _{0.846} Sn _{0.154}	0.5076	0.0924	1.20
Ge _{0.794} Sn _{0.206}	0.4764	0.1236	1.16

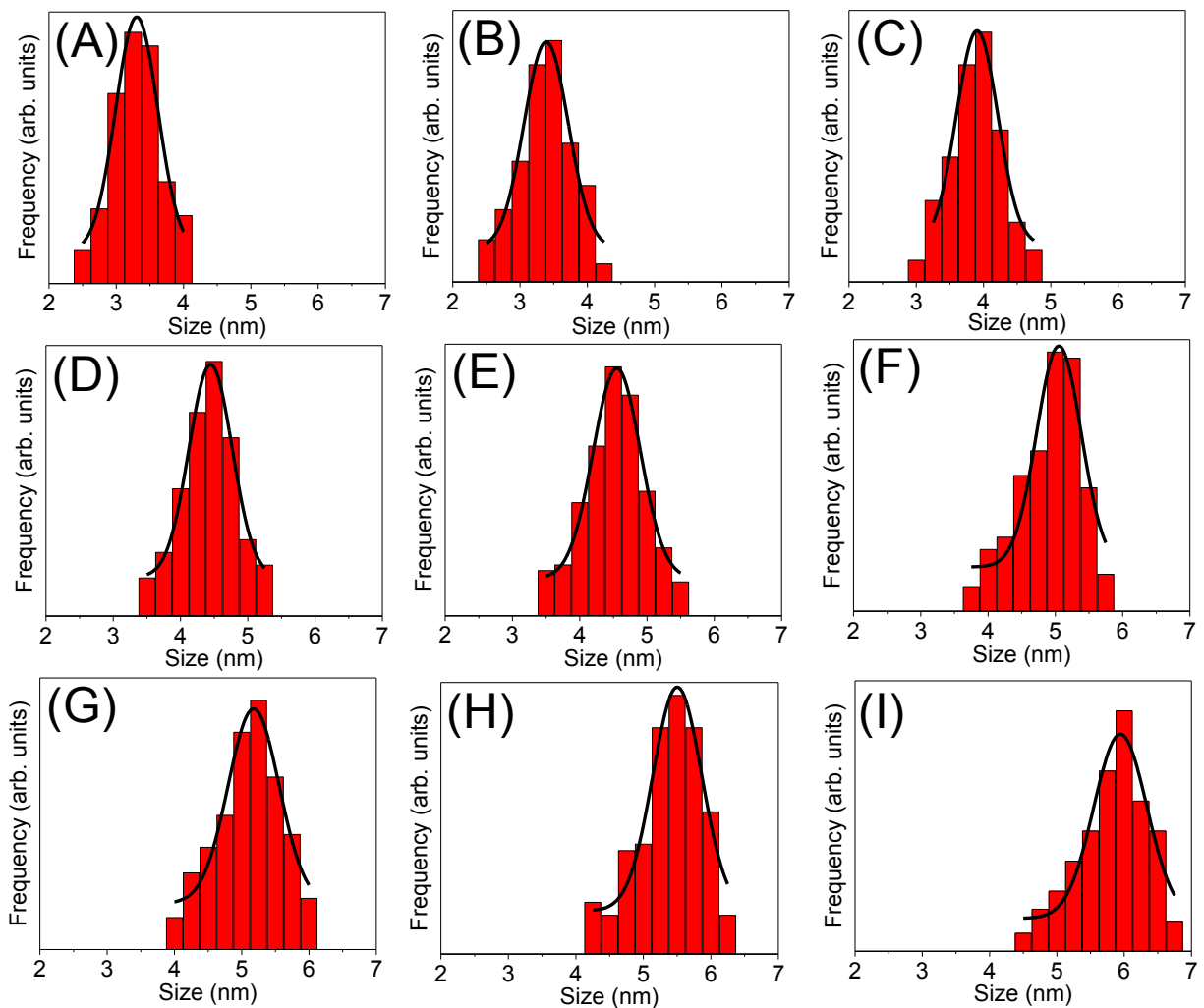


Figure S1. Size histograms of $\text{Ge}_{1-x}\text{Sn}_x$ alloy QDs with varying Sn composition: (A) $x = 1.5\%$, (B) $x = 2.7\%$, (C) $x = 4.2\%$, (D) $x = 5.6\%$, (E) $x = 7.9\%$, (F) $x = 9.1\%$, (G) $x = 11.2\%$, (H) $x = 15.4\%$, and (I) $x = 20.6\%$.

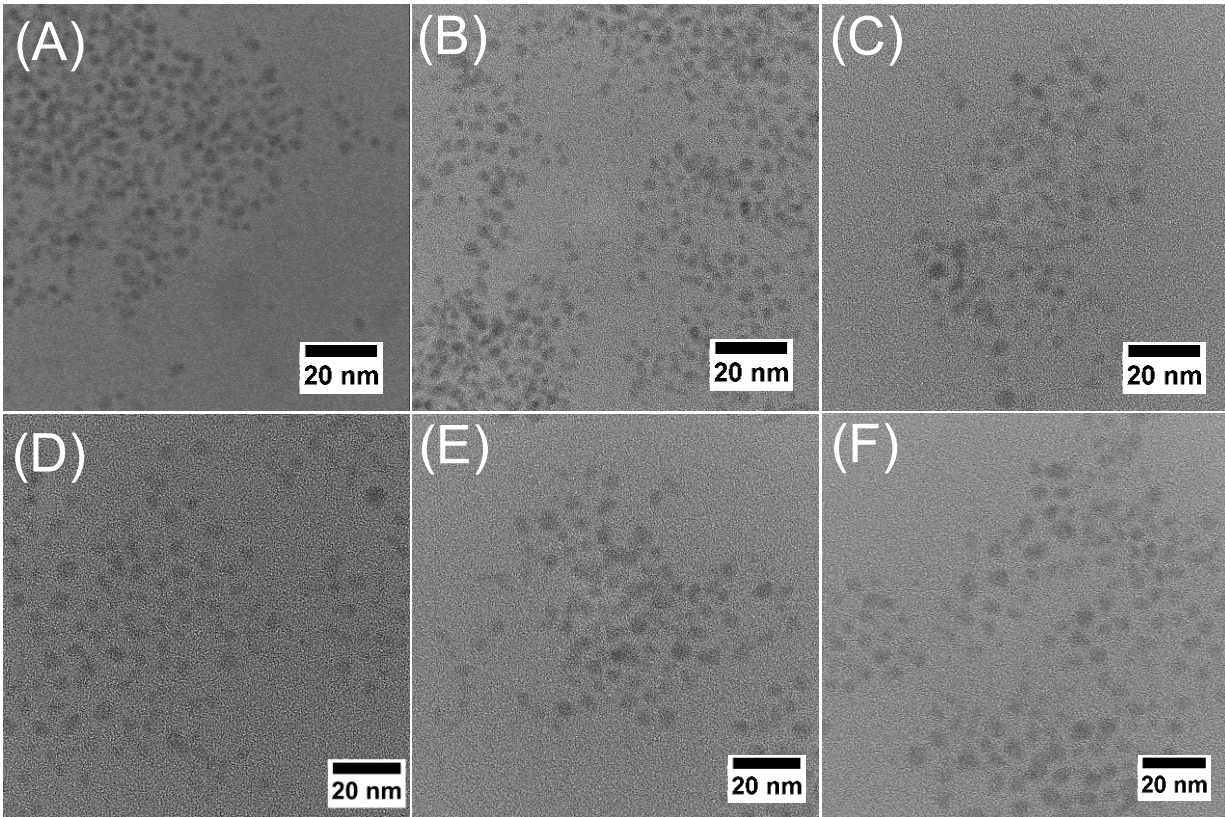


Figure S2. Representative TEM images of $\text{Ge}_{1-x}\text{Sn}_x$ alloy QDs with varying Sn composition: (A) $x = 2.7\%$, (B) $x = 5.6\%$, (C) $x = 7.9\%$, (D) $x = 11.2\%$, (E) $x = 15.4\%$, and (F) $x = 20.6\%$.

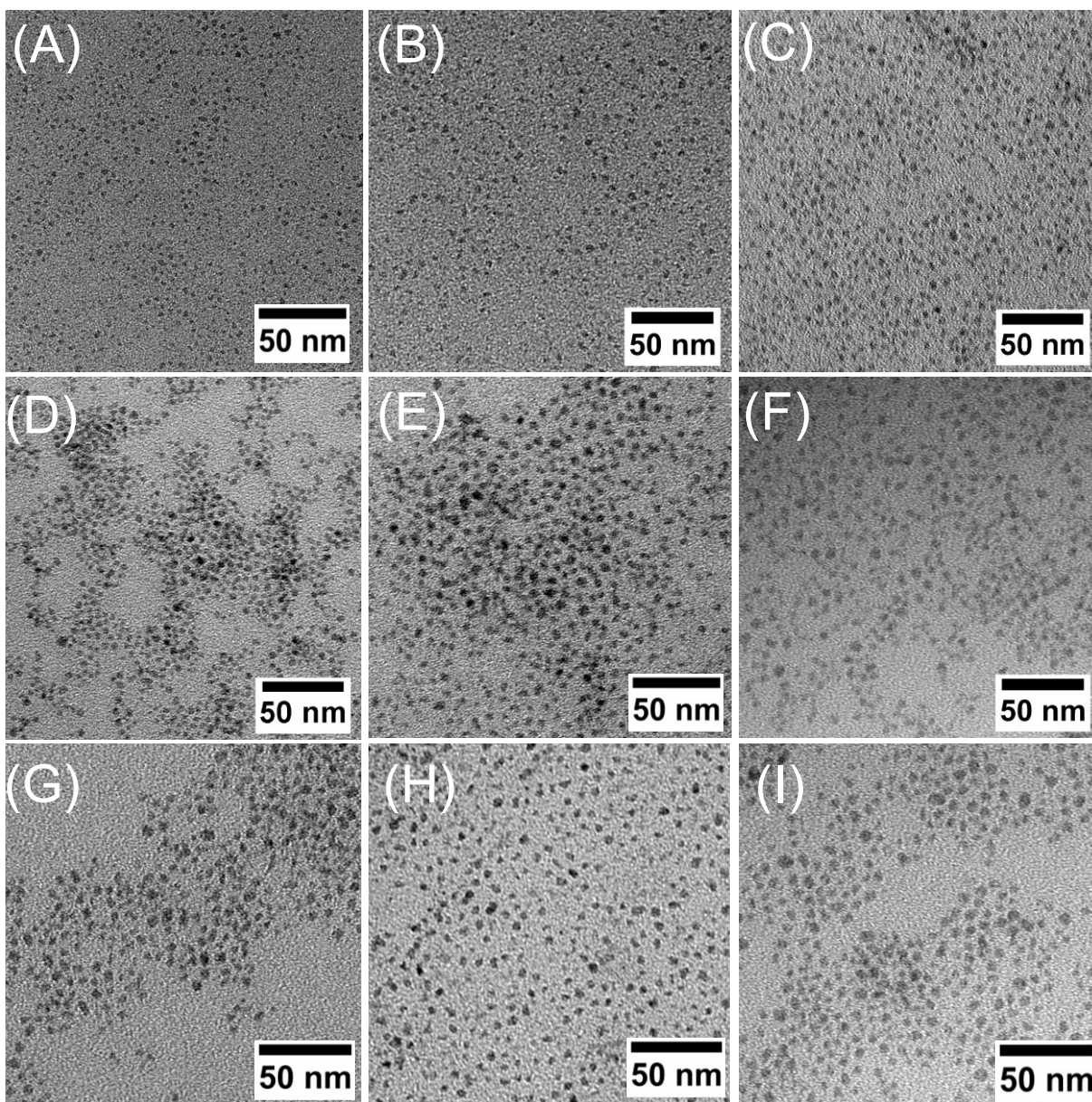


Figure S3. Representative low-resolution TEM images of $\text{Ge}_{1-x}\text{Sn}_x$ alloy QDs with varying Sn composition: (A) $x = 1.5\%$, (B) $x = 2.7\%$, (C) $x = 4.2\%$, (D) $x = 5.6\%$, (E) $x = 7.9\%$, (F) $x = 9.1\%$, (G) $x = 11.2\%$, (H) $x = 15.4\%$, and (I) $x = 20.6\%$.

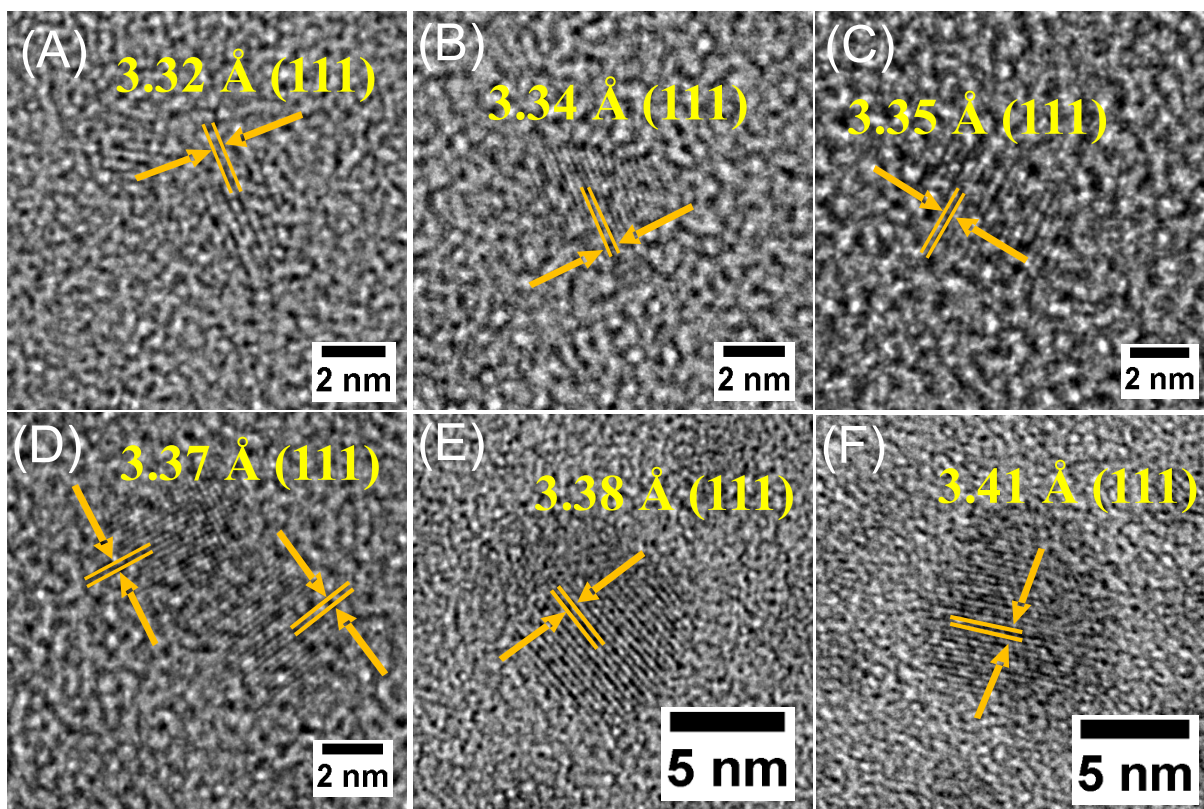


Figure S4. High resolution TEM images of Ge_{1-x}Sn_x alloy QDs displaying lattice fringes corresponding to expanded (111) plane of diamond cubic Ge: (A) $x = 2.7\%$ (B) $x = 5.6\%$, (C) $x = 7.9\%$, (D) $x = 11.2\%$, (E) $x = 15.4\%$, and (F) $x = 20.6\%$.

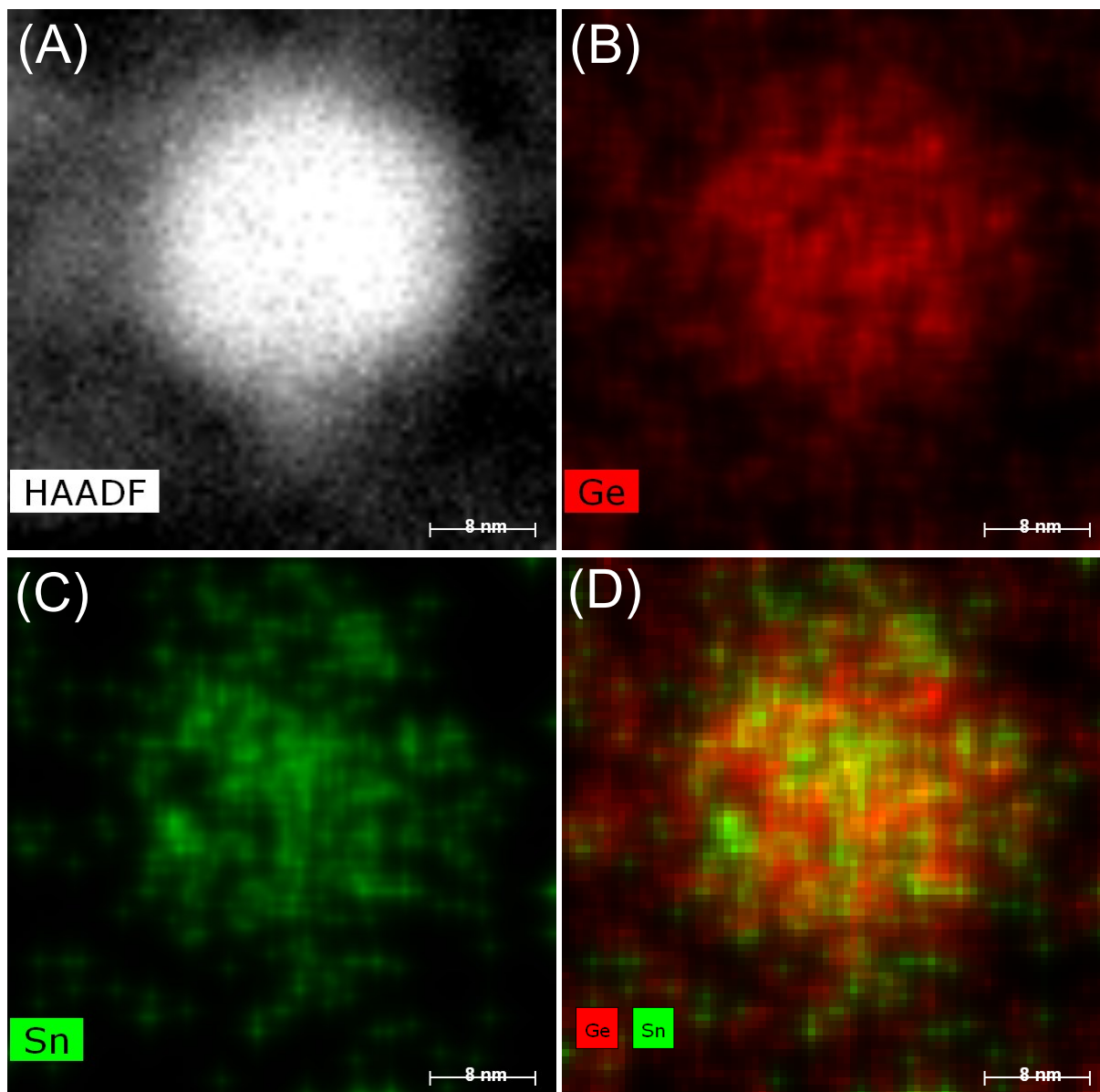


Figure S5. (A) Dark field TEM image of ~ 15 nm $\text{Ge}_{0.919}\text{Sn}_{0.091}$ alloy QD along with STEM/EDS elemental maps of (B) Ge, (C) Sn, and (D) an overlay of Ge and Sn, indicating the homogeneous distribution of elemental components throughout the alloy lattice.

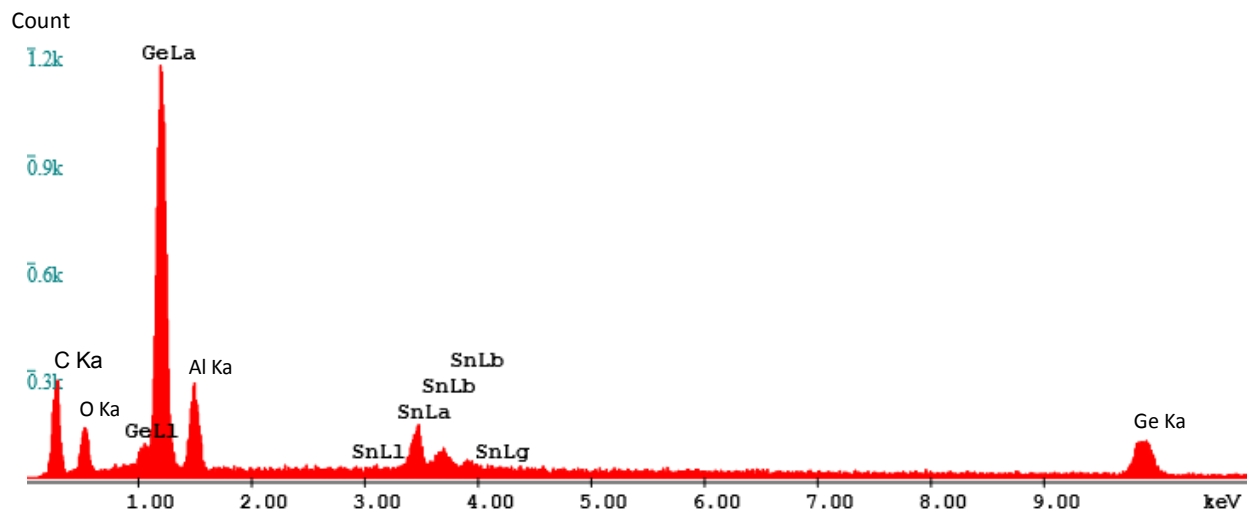


Figure S6. Representative SEM-EDS spectrum of $\text{Ge}_{0.909}\text{Sn}_{0.091}$ alloy QDs. The X-ray peak corresponding to aluminum (Al) is arising from sample holder.

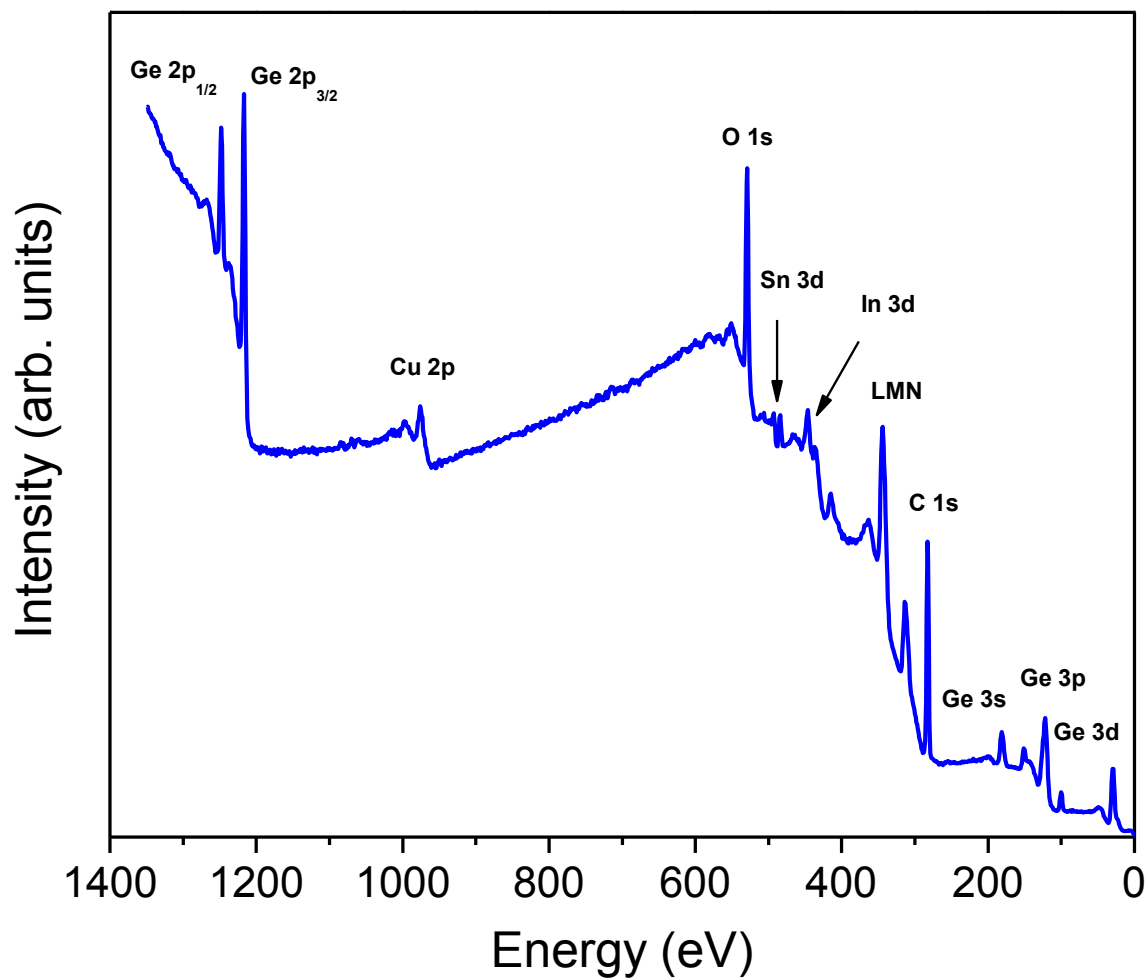


Figure S7. X-ray photoelectron spectra (survey scan) of $\text{Ge}_{0.888}\text{Sn}_{0.112}$ alloy QDs. Similar survey scans were obtained from QDs with other compositions.

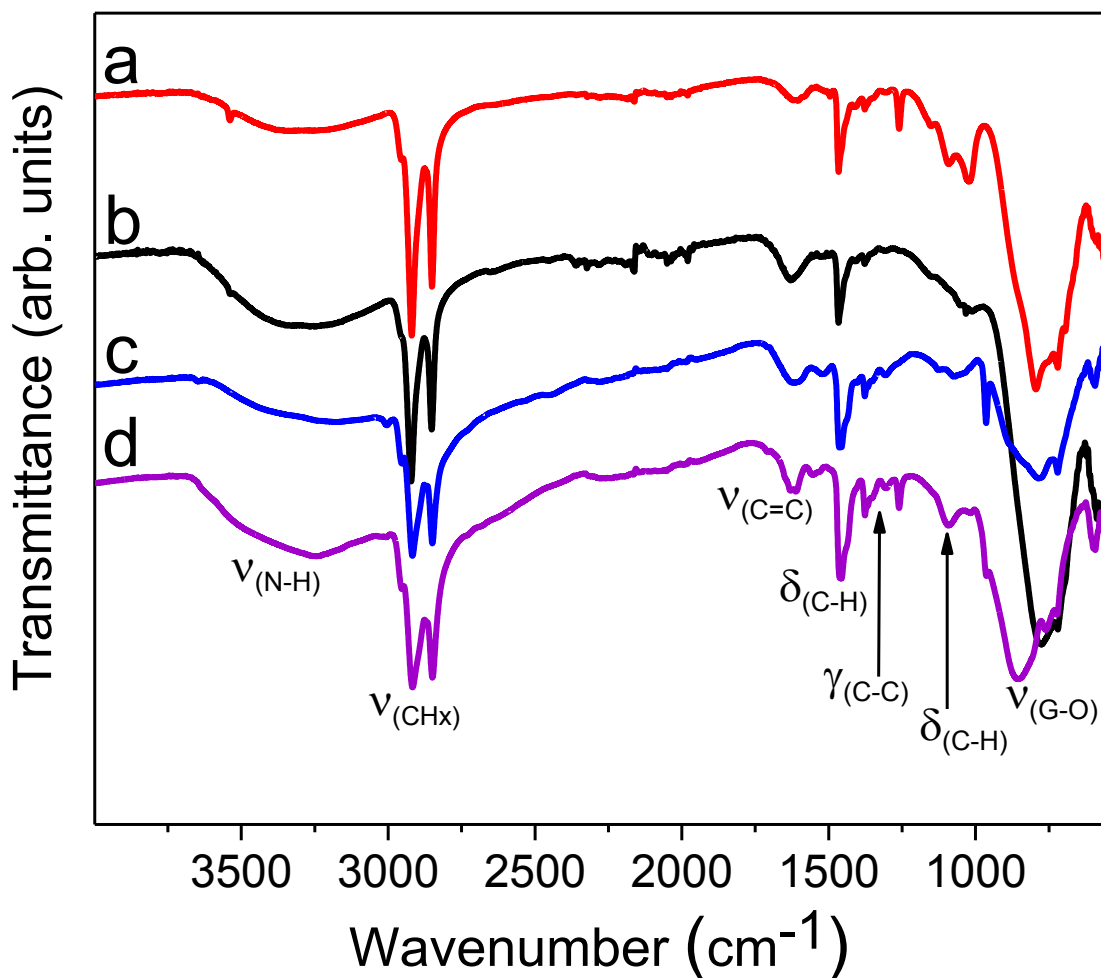


Figure S8. FT-IR spectra of $\text{Ge}_{1-x}\text{Sn}_x$ alloy QDs synthesized HDA/ODE. (a) $x = 0.015$, (b) $x = 0.056$, (c) $x = 0.112$, and (d) $x = 0.206$. The peaks at 2920 and 2850 cm^{-1} are arising from C–H asymmetric and symmetric stretching vibrations of alkyl chains, respectively.¹ The vibrations at 1361–1460 cm^{-1} corresponds to C–H bending $\delta_{(\text{CH}_x)}$ modes of alkyl chains.² A broader peak observed at 1622 cm^{-1} can be assigned to $\nu_{(\text{C}=\text{C})}$ whereas the weak band at ~ 3300 cm^{-1} can be attributed to $\nu_{(\text{N}-\text{H})}$ further indicating the presence of HDA on the QD surface. A broad band observed at 790–860 cm^{-1} can be attributed to $\nu_{(\text{Ge}-\text{O})}$ arising from adsorbed surface oxygen species¹, consistent with XPS O(1s) spectrum shown in Figure S9.

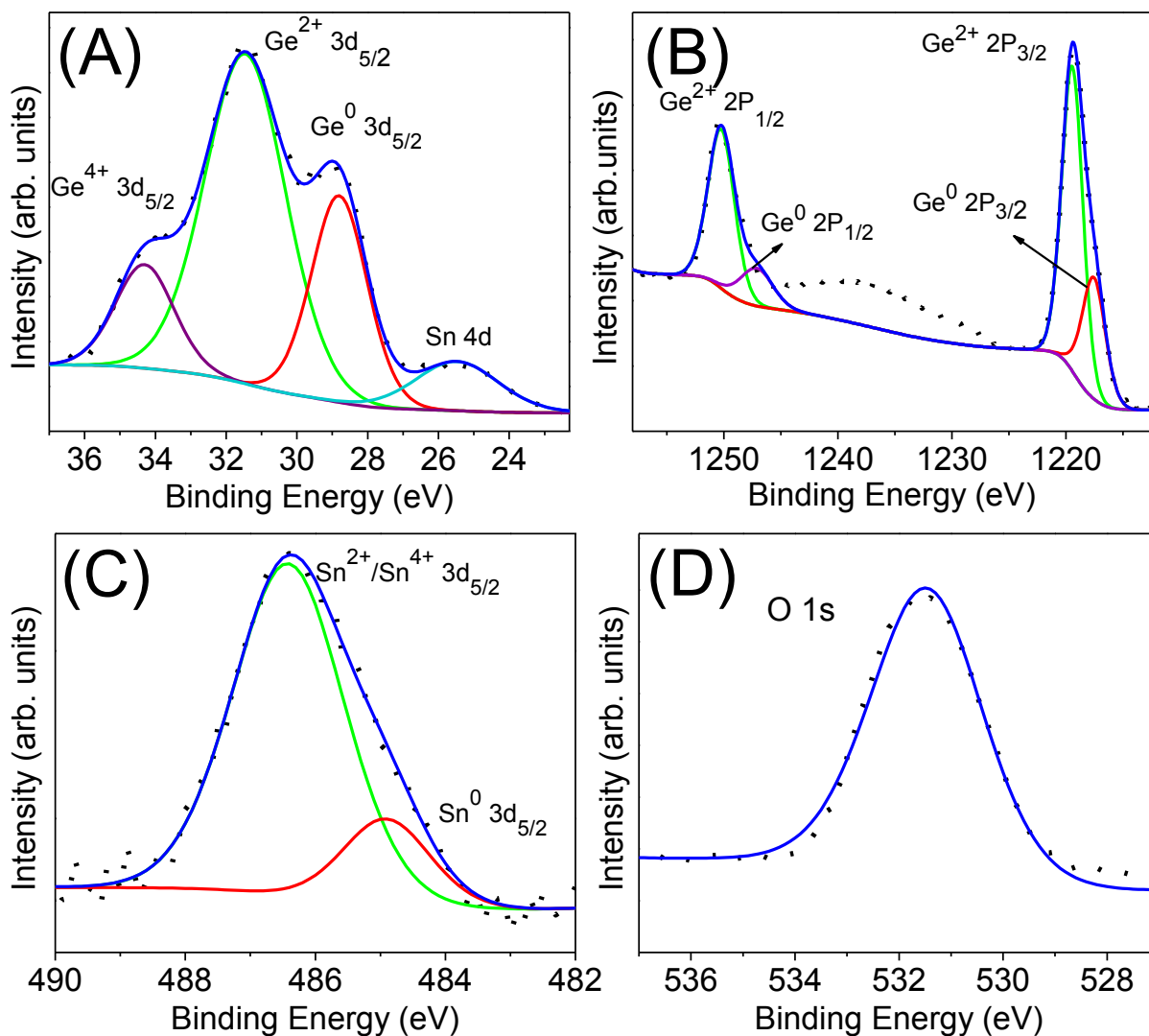


Figure S9. Representative X-ray photoelectron spectra of $\text{Ge}_{0.909}\text{Sn}_{0.091}$ alloy QDs displaying the (A) Ge(3d), (B) Ge(2P), (C) Sn(3d), and (D) O(1s) spectral regions. Dotted lines are spectral data, solid red and green lines are fitted deconvolutions, and blue lines are spectral envelopes. The peak at 531.5 eV in O(1s) spectrum corresponds to adsorbed H_2O .

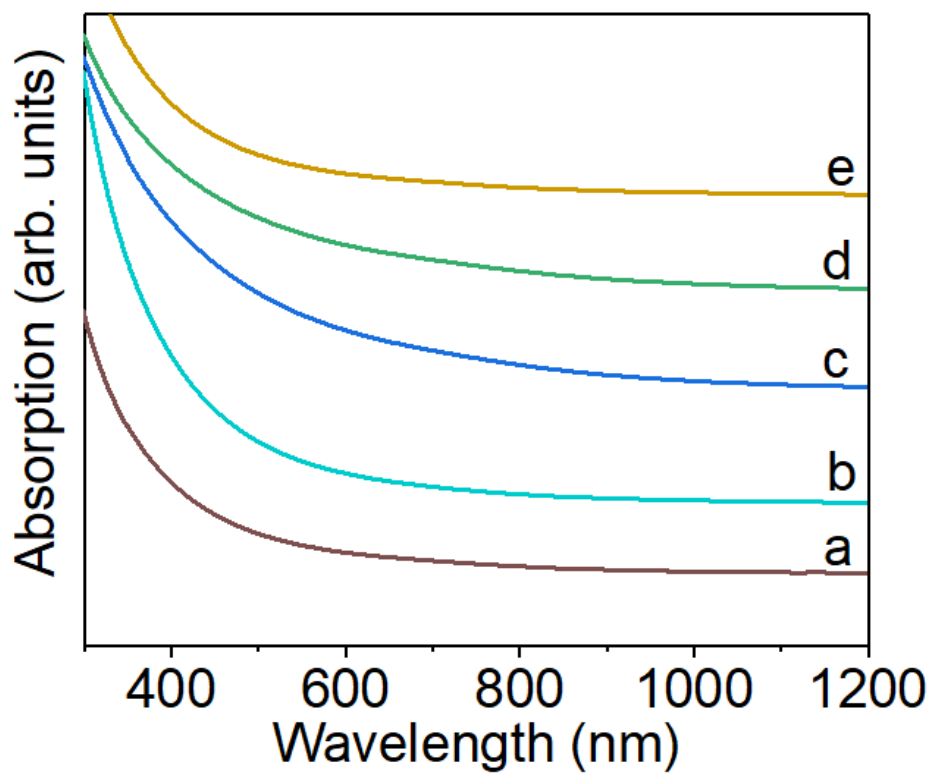


Figure S10. UV-visible-NIR absorption spectra of Ge_{1-x}Sn_x alloy QDs dispersed in CCl₄ as a function of Sn composition: (a) x = 1.5%, (b) x = 5.6%, (c) x = 9.1%, (d) x = 15.4%, and (e) x = 20.6%.

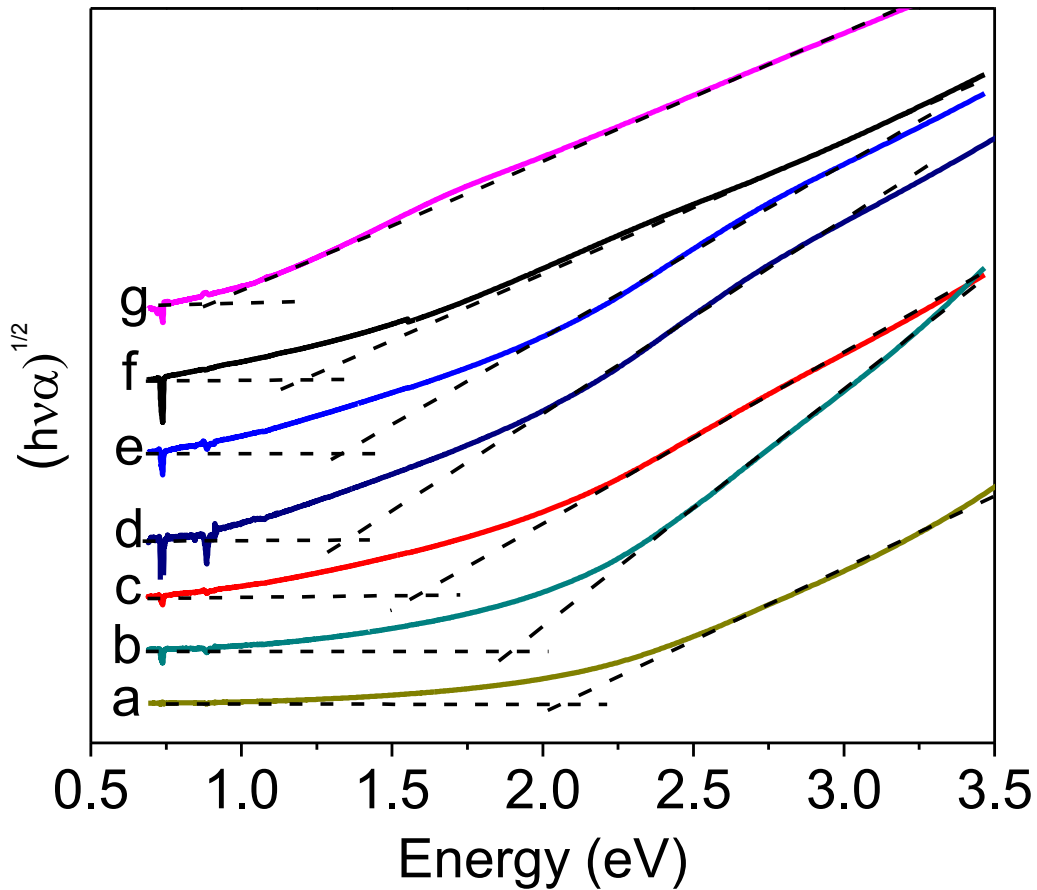


Figure S11. Solution absorption spectra (Tauc-indirect) of $\text{Ge}_{1-x}\text{Sn}_x$ alloy QDs as a function of Sn composition: (a) $x = 1.5\%$ (2.05 eV), (b) $x = 2.7\%$ (1.90 eV), (c) $x = 5.6\%$ (1.58 eV), (d) $x = 9.1\%$ (1.35 eV), (e) $x = 11.2\%$ (1.33 eV), (f) $x = 15.4\%$ (1.19 eV), and (g) $x = 20.6\%$ (0.90 eV). Corresponding energy gaps are shown in parentheses.

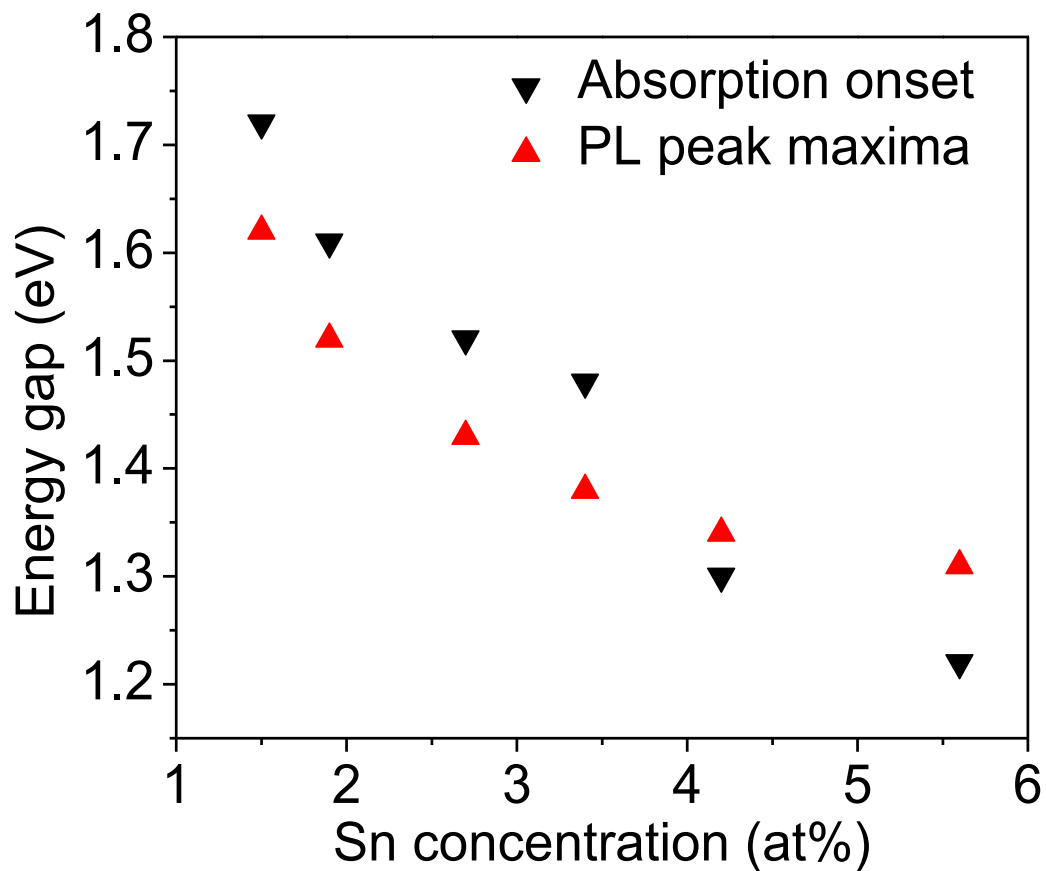


Figure S12. Experimental energy gaps of $3.2 \pm 0.2 - 5.7 \pm 0.5$ nm $\text{Ge}_{1-x}\text{Sn}_x$ alloy QDs as a function of Sn composition ($x = 1.5-5.6\%$). Data were obtained from room-temperature solid-state absorption and photoluminescence (PL) studies.

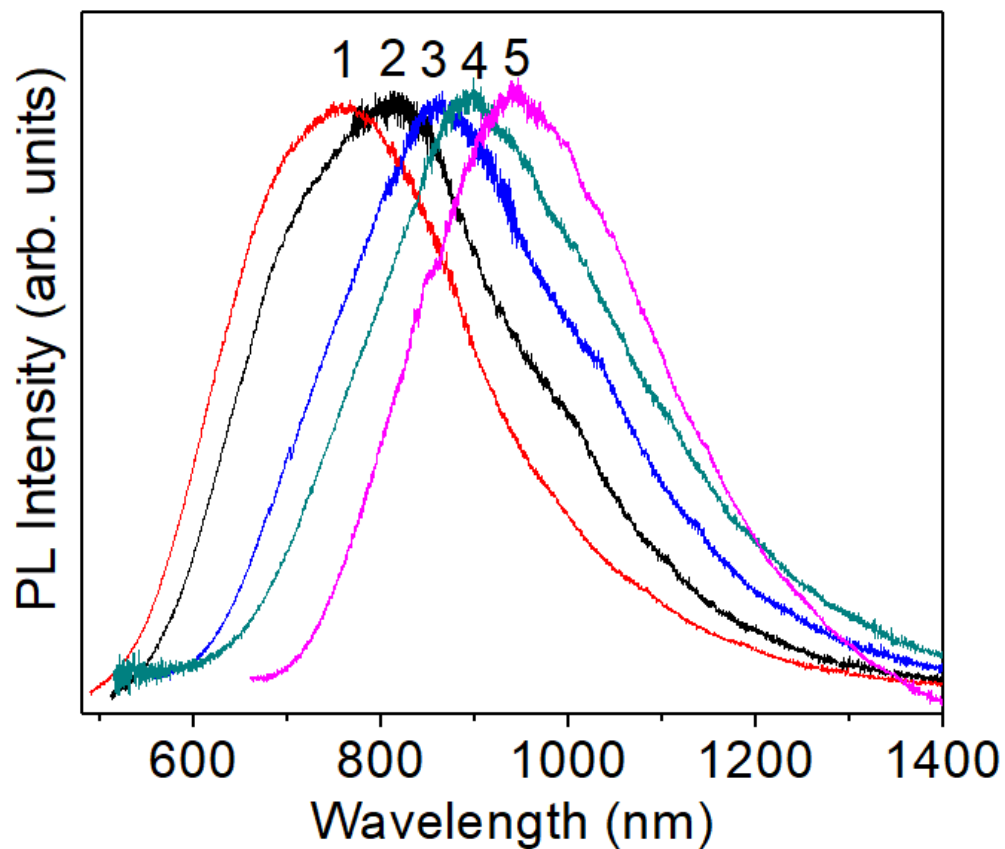


Figure S13. Room-temperature solution-state photoluminescence spectra of Ge_{1-x}Sn_x alloy QDs with varying Sn composition (1) $x = 1.5\%$ (760 nm), (2) $x = 1.9\%$ (812 nm), (3) $x = 2.7\%$ (860 nm), (4) $x = 3.5\%$ (895 nm), and (5) $x = 5.6\%$ (940 nm). Corresponding PL peak maxima are shown in parentheses.

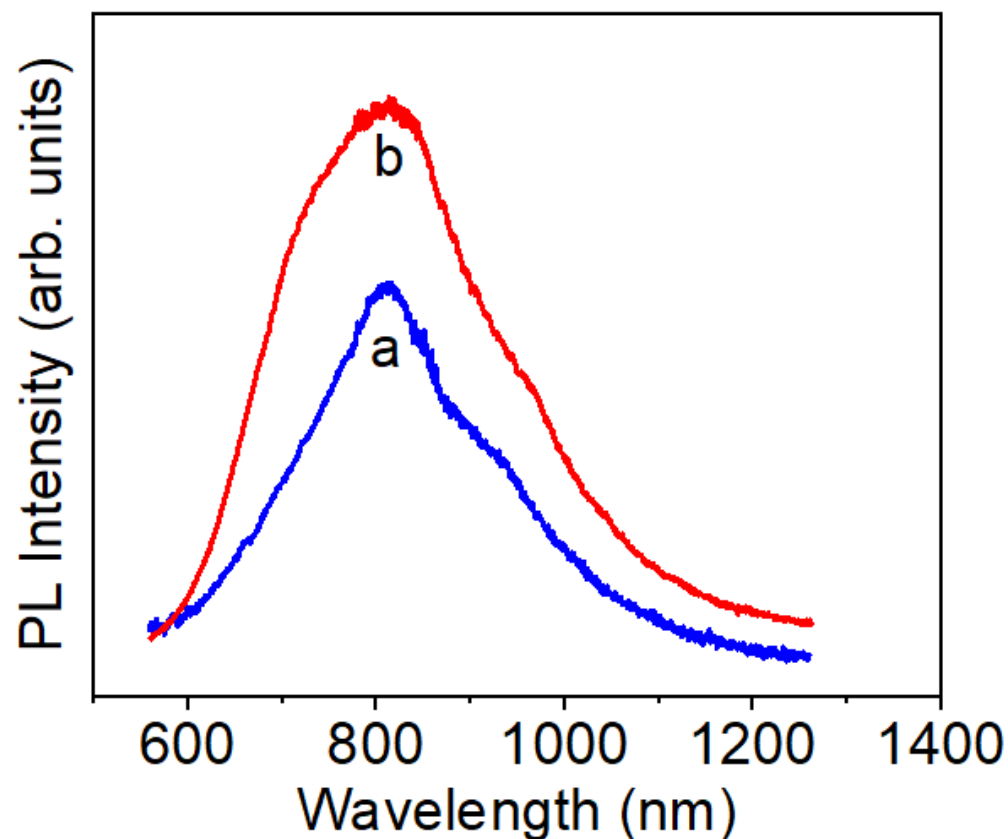


Figure S14. Room-temperature solution-state photoluminescence spectra of Ge_{0.98}Sn_{0.02} alloy QDs with varying excitation wavelengths: (a) 350 nm and (b) 485 nm show no peak shift observed with varying excitation wavelength. The solution-state PL spectra are slightly weaker than those reordered from solid-state samples because of lower excitation powder used in the solution-state analysis. However, both solution-state and solid-state PL spectra show consistent PL peak maxima with varying excitation energy, suggesting that emission results from inter-band electronic transitions of alloy QDs.³

References:

- (1) B. M. Nolan, E. K. Chan, X. Zhang, E. Muthuswamy, K. V. Benthem, S. M. Kauzlarich, *ACS Nano* 2016, **10**, 5391–5397.
- (2) G. T. Chandrappa, J. Livage, *Synth. React. Inorg., Met.-Org., Nano-Met. Chem.* 2006, **36**, 23–28.
- (3) P. Xiao, J. Lou, H. Zhang, W. Song, X.-L. Wu, H. Lin, J. Chen, S. Liuc, X. Wang, *Catal. Sci. Technol.*, 2018, **8**, 201–209.